ELSEVIER

Journal of Quantitative Spectroscopy & Radiative Transfer 100 (2006) 268–276

Journal of Quantitative Spectroscopy & Radiative Transfer

www.elsevier.com/locate/jqsrt

Far-field approximation in electromagnetic scattering

Michael I. Mishchenko*

NASA Goddard Institute for Space Studies, 2880 Broadway, New York, NY 10025, USA

Abstract

The volume integral equation formalism is used to derive and analyze specific criteria of applicability of the far-field approximation in electromagnetic scattering by a finite three-dimensional object. In the case of wavelength-sized and larger objects, this analysis leads to a natural subdivision of the entire external space into a near-field zone, a transition zone, and a far-field zone. It is demonstrated that the general criteria of far-field scattering are consistent with the theory and practice of *T*-matrix computations.

Keywords: Electromagnetic scattering; Scattering by particles; Far-field approximation

1. Introduction

It is well known that in the so-called far-field zone of a fixed finite object, the propagation of the scattered electromagnetic wave is away from the object [1]. Furthermore, the electric and magnetic field vectors vibrate in the plane perpendicular to the propagation direction and their amplitudes decay inversely with distance from the object. The tranversality of both the incident plane wave and the scattered outgoing spherical wave allows one to introduce the concept of the amplitude scattering matrix [2] as well as to define the corresponding sets of Stokes parameters and describe the response of a well-collimated polarization-sensitive detector of light in terms of the 4×4 so-called phase and extinction matrices [3].

These attractive features have led to the widespread use of the far-field approximation (FFA) [2–11] and have made it a cornerstone of the microphysical approach to radiative transfer [12,13]. However, one must always keep in mind that for an observation point to be in the far-field zone of an object its distance from the object must satisfy certain inequalities. These inequalities were derived in [14], but their physical meaning and practical implications were not analyzed. Hence the objective of this tutorial paper is to perform such an analysis. We will accomplish this objective through a modified way of deriving the FFA formulas which will make especially transparent the specific role of each far-field criterion.

In order to save space and avoid redundancy, we will take advantage of the on-line availability of [3] and will use exactly the same terminology and notation.

*Corresponding author. Tel.: +1 212 678 5590; fax: +1 212 678 5622.
E-mail address: crmim@giss.nasa.gov.

0022-4073/$ - see front matter
doi:10.1016/j.jqsrt.2005.11.044

2. Far-field approximation

As in Chapter 2 of [3], we consider a finite scattering object in the form of an arbitrary body embedded in an infinite, homogeneous, linear, isotropic, and nonabsorbing medium. The interior of the particle is assumed to be filled with an isotropic, linear, and possibly inhomogeneous material (Fig. 1). We start off where Section 2.1 of [3] ends, subdivide the scattering object into a large number of elementary volume elements ΔV, and rewrite Eq. (2.16) of [3] for an external observation point $\mathbf{r}$ in the following discrete form:

$$\mathbf{E}^{\rm sca}(\mathbf{r}) = \frac{k_1^2}{4\pi} \lim_{\Delta V \to 0} \sum_i \Delta V (\mathsf{m}_i^2 - 1) \left(\overleftrightarrow{I} + \frac{1}{k_1^2} \nabla \otimes \nabla \right) \cdot \mathbf{E}_i \frac{\exp(ik_1 \rho_i)}{\rho_i}, \quad \mathbf{r} \in V_{\rm EXT}, \tag{1}$$

where the index i numbers the volume elements, $\mathbf{E}_i$ and m_i are the electric field and relative refractive index values, respectively, at the center of the ith volume element, $\rho_i = |\boldsymbol{\rho}_i|$ is the distance from the center of the ith volume element to the observation point, $\boldsymbol{\rho}_i = \mathbf{r} - \mathbf{r}_i$ is the vector connecting the center of the ith volume element and the observation point, and $\mathbf{r}_i$ is the radius-vector of the center of the ith volume element (Fig. 2). Recall now that in spherical polar coordinates (r, θ, φ)

$$\nabla = \hat{\mathbf{r}} \frac{\partial}{\partial r} + \hat{\boldsymbol{\theta}} \frac{1}{r} \frac{\partial}{\partial \theta} + \hat{\boldsymbol{\varphi}} \frac{1}{r \sin\theta} \frac{\partial}{\partial \varphi}, \tag{2}$$

$$\frac{\partial}{\partial r} \hat{\mathbf{r}} = 0, \quad \frac{\partial}{\partial \theta} \hat{\mathbf{r}} = \hat{\boldsymbol{\theta}}, \quad \frac{\partial}{\partial \varphi} \hat{\mathbf{r}} = \hat{\boldsymbol{\varphi}} \sin\theta, \tag{3}$$

where the order of operator components relative to $\hat{\mathbf{r}}$, $\hat{\boldsymbol{\theta}}$, and $\hat{\boldsymbol{\varphi}}$ in Eq. (2) is essential because the unit basis vectors depend on θ and φ. The simplicity of these formulas makes it convenient to evaluate the contribution of each volume element to the sum on the right-hand side of Eq. (1) by using a local coordinate system originating at the center of this volume element and having the same orientation as the laboratory reference

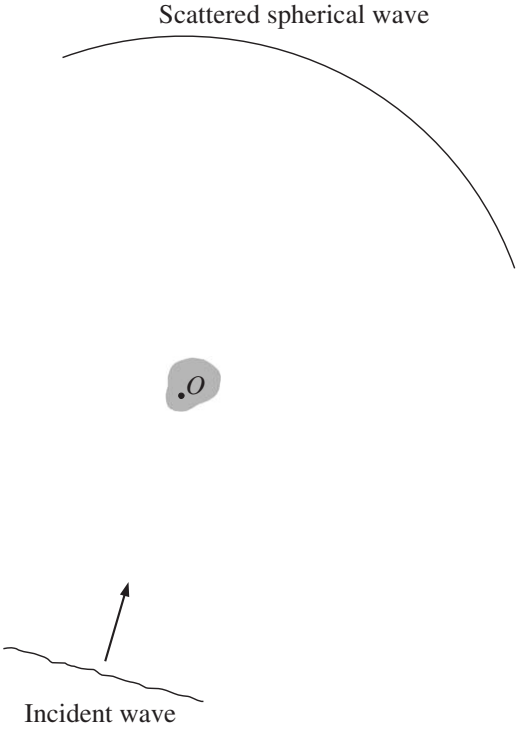

Fig. 1. Schematic representation of the electromagnetic scattering problem. The unshaded exterior region $V_{\rm EXT}$ is unbounded in all directions, whereas the shaded area represents the interior region $V_{\rm INT}$.

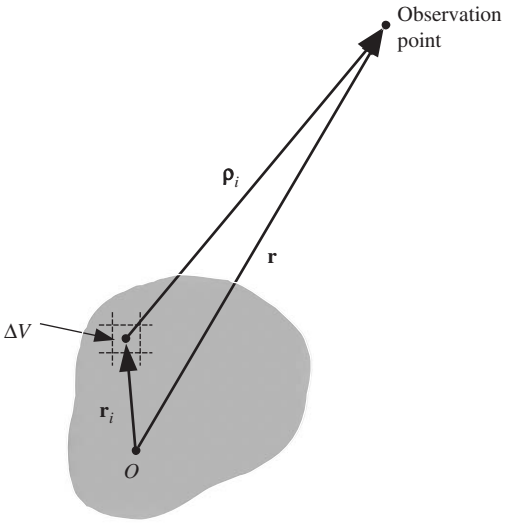

Fig. 2. Derivation of Eq. (5).

frame. This is done by making the substitution $\mathbf{r} \to \boldsymbol{\rho}_i$ for each new i. Recalling that

$$\nabla \cdot (f\mathbf{a}) = f\nabla \cdot \mathbf{a} + \mathbf{a} \cdot \nabla f$$

and

$$\nabla \frac{\exp(\pm ikr)}{r} = \left(\pm ik - \frac{1}{r}\right)\frac{\exp(\pm ikr)}{r}\hat{\mathbf{r}}$$

and assuming that

$$k_1\rho_i \gg 1 \quad \text{for any } i \tag{4}$$

then yield

$$\mathbf{E}^{\text{sca}}(\mathbf{r}) = \frac{k_1^2}{4\pi}\lim_{\Delta V\to 0}\sum_i \Delta V(\mathsf{m}_i^2 - 1)\frac{\exp(ik_1\rho_i)}{\rho_i}(\overleftrightarrow{I} - \hat{\boldsymbol{\rho}}_i \otimes \hat{\boldsymbol{\rho}}_i)\cdot \mathbf{E}_i, \quad \mathbf{r} \in V_{\text{EXT}}, \tag{5}$$

where $\hat{\boldsymbol{\rho}}_i = \boldsymbol{\rho}_i/\rho_i$ is the unit vector originating at the center of the ith volume element and directed towards the observation point. Finally,

$$\mathbf{E}^{\text{sca}}(\mathbf{r}) = \frac{k_1^2}{4\pi}\int_{V_{\text{INT}}} d\mathbf{r}'[\mathsf{m}^2(\mathbf{r}') - 1]\frac{\exp(ik_1|\mathbf{r} - \mathbf{r}'|)}{|\mathbf{r} - \mathbf{r}'|}(\overleftrightarrow{I} - \hat{\boldsymbol{\rho}}' \otimes \hat{\boldsymbol{\rho}}')\cdot \mathbf{E}(\mathbf{r}'), \quad \mathbf{r} \in V_{\text{EXT}}, \tag{6}$$

where

$$\hat{\boldsymbol{\rho}}' = \frac{\mathbf{r} - \mathbf{r}'}{|\mathbf{r} - \mathbf{r}'|}. \tag{7}$$

Eq. (6) has two important implications. First, it shows that the scattered field at an external observation point is a vector superposition of partial scattered fields (wavelets), which are created by infinitesimal volume elements constituting the interior of the object. Second, it demonstrates that each wavelet is an outgoing transverse spherical wave (Fig. 3). Indeed, the identity dyadic in spherical polar coordinates is given by

$$\overleftrightarrow{I} = \hat{\mathbf{r}} \otimes \hat{\mathbf{r}} + \hat{\boldsymbol{\theta}} \otimes \hat{\boldsymbol{\theta}} + \hat{\boldsymbol{\varphi}} \otimes \hat{\boldsymbol{\varphi}}.$$

Therefore, the dyadic factor

$$\overleftrightarrow{I} - \hat{\boldsymbol{\rho}}' \otimes \hat{\boldsymbol{\rho}}'$$

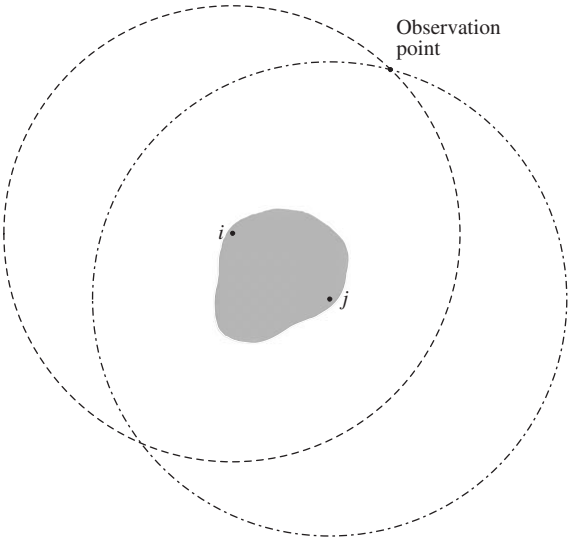

Fig. 3. Spherical wavelets generated by infinitesimal volume elements centered at points i (dashed line) and j (dot-dashed line).

in Eq. (6) ensures that each wavelet is transverse, i.e., the electric field vector of the wavelet at the observation point is perpendicular to its propagation direction $\hat{\boldsymbol{\rho}}'$:

$$\hat{\boldsymbol{\rho}}' \cdot (\overleftrightarrow{I} - \hat{\boldsymbol{\rho}}' \otimes \hat{\boldsymbol{\rho}}') \cdot \mathbf{E}(\mathbf{r}') = 0. \tag{8}$$

Furthermore, the electric field of the wavelet decays inversely with distance $|\mathbf{r} - \mathbf{r}'|$ from the center of the infinitesimal volume element.

Let us now assume that the origin of the laboratory coordinate system O is inside the scattering object (Figs. 1 and 4). Usually one is interested in calculating the scattered field in the so-called far-field zone of the entire object. Specifically, assuming that the distance r from the origin to the observation point is much greater than any linear dimension of the scatterer,

$$r \gg r' \quad \text{for any } \mathbf{r}' \in V_{\mathrm{INT}}, \tag{9}$$

we have

$$\overleftrightarrow{I} - \hat{\boldsymbol{\rho}}' \otimes \hat{\boldsymbol{\rho}}' \approx \overleftrightarrow{I} - \hat{\mathbf{r}} \otimes \hat{\mathbf{r}}, \tag{10}$$

$$|\mathbf{r} - \mathbf{r}'| = r\sqrt{1 - 2\frac{\hat{\mathbf{r}} \cdot \mathbf{r}'}{r} + \frac{r'^2}{r^2}} \approx r - \hat{\mathbf{r}} \cdot \mathbf{r}' + \frac{r'^2}{2r}, \tag{11}$$

where $\hat{\mathbf{r}} = \mathbf{r}/r$ is the unit vector in the direction of $\mathbf{r}$, Fig. 4. The last two terms on the right-hand side of Eq. (11) can be neglected in computing the slowly varying denominator in the expression on the right-hand side of Eq. (6), thereby yielding

$$\frac{1}{|\mathbf{r} - \mathbf{r}'|} \approx \frac{1}{r}, \tag{12}$$

but not in computing the rapidly oscillating factor $\exp(\mathrm{i}k_1|\mathbf{r} - \mathbf{r}'|)$. Assuming, however, that

$$\frac{k_1 r'^2}{2r} \ll 1 \quad \text{for any } \mathbf{r}' \in V_{\mathrm{INT}}, \tag{13}$$

we finally obtain

$$\mathbf{E}^{\mathrm{sca}}(\mathbf{r}) \approx \frac{\exp(\mathrm{i}k_1 r)}{r}\frac{k_1^2}{4\pi}(\overleftrightarrow{I} - \hat{\mathbf{r}} \otimes \hat{\mathbf{r}}) \cdot \int_{V_{\mathrm{INT}}} \mathrm{d}\mathbf{r}'[\mathsf{m}^2(\mathbf{r}') - 1]\mathbf{E}(\mathbf{r}') \exp(-\mathrm{i}k_1 \hat{\mathbf{r}} \cdot \mathbf{r}'). \tag{14}$$

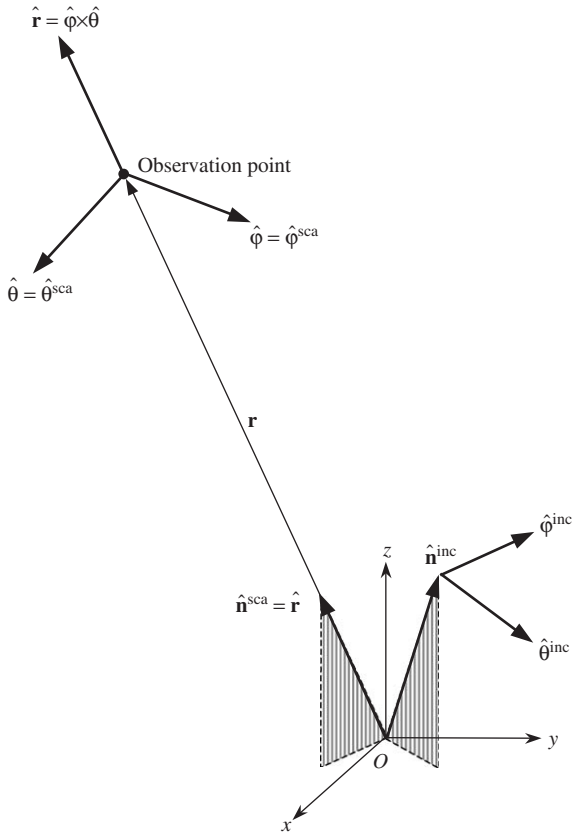

Fig. 4. Scattering in the far-field zone of the entire object.

This remarkable formula is the main result of the FFA and demonstrates that the scattered electric field at a large distance from the object behaves as a single outgoing transverse spherical wave centered at O and propagating in the direction of the radial unit vector $\hat{\mathbf{r}}$. Indeed, the scattered field decays inversely with distance r from the origin and

$$\hat{\mathbf{r}} \cdot \mathbf{E}^{\rm sca}(\mathbf{r}) = 0. \tag{15}$$

Thus, only the θ- and φ-component of the electric vector of the scattered field are non-zero. Eq. (14) can be rewritten in the form

$$\mathbf{E}^{\rm sca}(\mathbf{r}) = \frac{\exp(ik_1 r)}{r}\mathbf{E}_1^{\rm sca}(\hat{\mathbf{r}}), \quad \hat{\mathbf{r}} \cdot \mathbf{E}_1^{\rm sca}(\hat{\mathbf{r}}) = 0, \tag{16}$$

where the vector $\mathbf{E}_1^{\rm sca}(\hat{\mathbf{r}})$ is independent of r and describes the angular distribution of the scattered radiation in the far-field zone.

3. Criteria of the far-field approximation

Let a be the radius of the smallest circumscribing sphere of the scattering object centered at O. Then the criteria (4), (9), and (13) of the FFA can be summarized as follows:

$$k_1(r-a) \gg 1, \tag{17}$$

$$r \gg a \quad \text{or} \quad k_1 r \gg k_1 a, \tag{18}$$

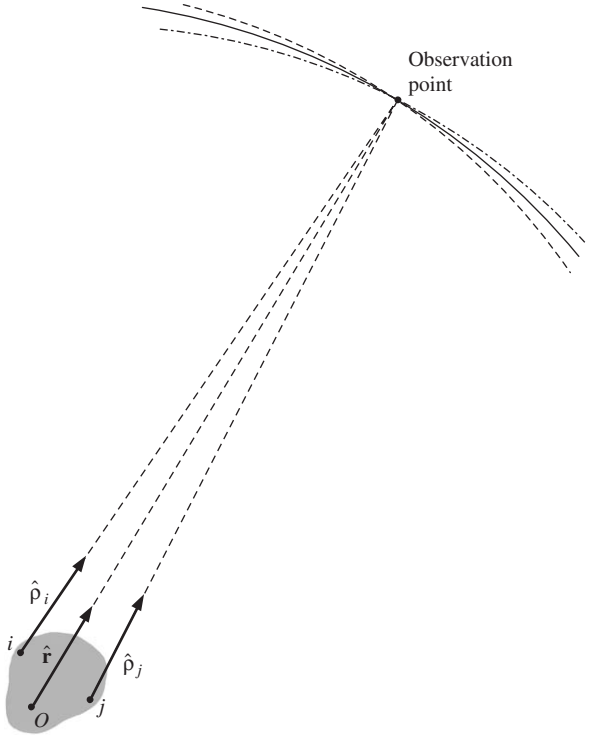

Fig. 5. The individual spherical wavefronts generated by infinitesimal volume elements centered at points i (dashed curve) and j (dot-dashed curve) nearly merge with increasing distance of the observation point from the scattering object and become locally indistinguishable from the unified spherical wavefront centered at the common origin (solid curve). The respective propagation directions at the observation point also become close and eventually coincide.

$$r \gg \frac{k_1 a^2}{2} \quad \text{or} \quad k_1 r \gg \frac{k_1^2 a^2}{2}. \tag{19}$$

Inequality (17) means that the distance from any point inside the object to the observation point must be much greater than the wavelength. This ensures that at the observation point, the partial field scattered by any differential volume element develops into an outgoing spherical wavelet.

Inequality (18) requires the observation point to be located at a distance from the object much greater than the object's size. This ensures that when the partial wavelets generated by the elementary volume elements constituting the object arrive at the observation point, they propagate in essentially the same scattering direction, Fig. 5, and are equally attenuated by the factor 1/distance:

$$\frac{\mathbf{r}-\mathbf{r}'}{|\mathbf{r}-\mathbf{r}'|} \approx \hat{\mathbf{r}} \quad \text{and} \quad \frac{1}{|\mathbf{r}-\mathbf{r}'|} \approx \frac{1}{r} \quad \text{for any } \mathbf{r}' \in V_{\text{INT}}. \tag{20}$$

The meaning of inequality (19) is a bit more subtle, but becomes clear from the inspection of Fig. 6, in which the observation point is shown relative to the smallest circumscribing sphere of the object. The phase difference between the straight path connecting the observation point and a point on the sphere surface and the path connecting the observation point and the origin is given by

$$k_1(r'-r) \approx \frac{k_1 a^2}{2r} - k_1 a \cos\varsigma. \tag{21}$$

The second term on the right-hand side of this expression is independent of r (for a fixed scattering direction), whereas the variation of the first term with changing r is significant unless $k_1 a^2/2r \ll 1$. Therefore, we can interpret the inequality (19) as the requirement that the observation point be so far from the scatterer that the phase difference between the paths connecting the observation point and any two points of the scatterer

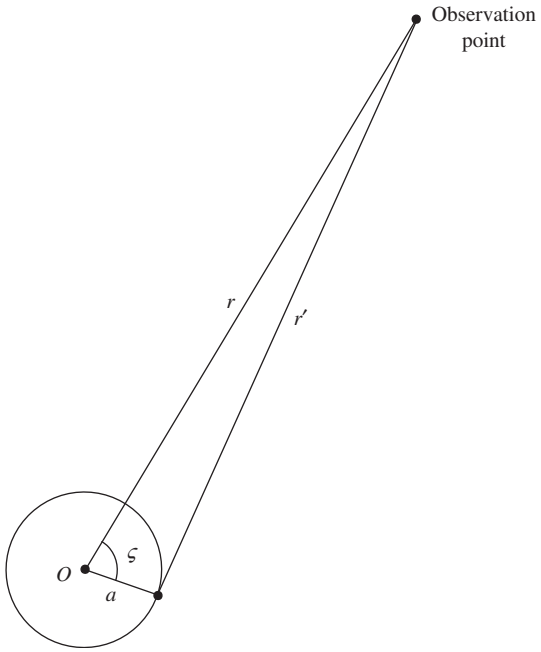

Fig. 6. Interpretation of the inequality (19).

becomes independent of r for any fixed scattering direction. As a consequence, the surfaces of constant phase of the partial wavelets generated by the elementary volume elements constituting the object coincide locally when they reach an observation point situated in the far-field zone, and the wavelets form a single outgoing spherical wave (compare Figs. 3 and 5). This implies that the entire scatterer is effectively treated as a point-like body located at the origin of the laboratory coordinate system.

In view of inequality (18), inequality (17) can be simplified:

$$k_1 r \gg 1. \tag{22}$$

Furthermore, all three criteria of far-field scattering can be written as the following single inequality:

$$k_1 r \gg \max(1, \tfrac{1}{2}x^2), \tag{23}$$

where $x = k_1 a$ is the dimensionless so-called size parameter of the object.

3. Discussion

It is remarkable that all three far-field criteria (17)–(19) are purely geometrical and do not involve the particle refractive index. The relative importance of these criteria changes with particle size relative to the wavelength. For particles much smaller than the wavelength ($k_1 a \ll 1$), inequality (17) is the most restrictive of the three. When the size parameter $k_1 a$ is of order unity, all three criteria are roughly equivalent. For particles much greater than the wavelength ($k_1 a \gg 1$), inequality (19) becomes the most demanding and can "move" the far-field zone much farther from the particle than the other two inequalities.

For particles comparable to and greater than the incident wavelength, the above derivation and discussion suggest the existence of three distinct zones (Fig. 7). In the far-field zone, all three criteria (17)–(19) are satisfied and the total scattered field is a unified outgoing spherical wave. Each point of the transition zone satisfies inequality (4) but not inequalities (18) and (19). Therefore, although the total scattered field is not a unified spherical wave, it can still be represented as a superposition of outgoing spherical wavelets generated by the elementary volume elements of the object. In the near-field zone, all three criteria (17)–(19) are violated, and the total scattered field does not have a simple representation.

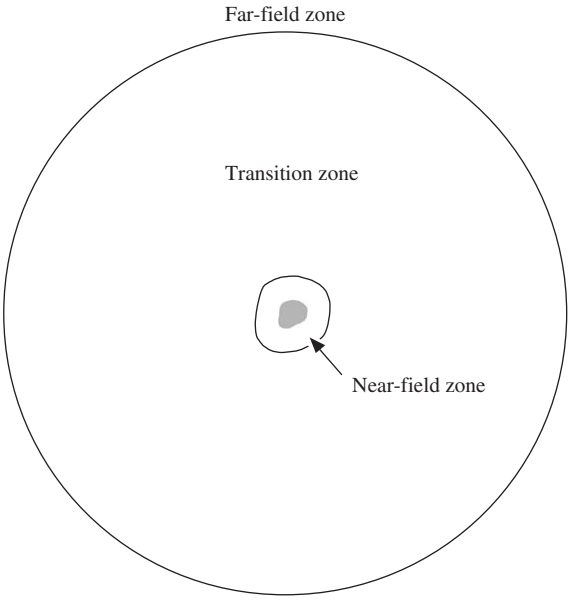

Fig. 7. Near-field, transition, and far-field zones.

For objects with sizes smaller than the wavelength, the transition zone is absent.

The far-field criteria (17)–(19) are consistent with the theory and practice of T-matrix computations. Indeed, Eqs. (5.3), (C.30), and (C.31) of [3] imply that expression (5.9) for the amplitude of the far-zone electric field $\mathbf{E}_1^{\rm sca}$ and, thus, expression (5.10) for the scattering dyadic and expressions (5.11)–(5.14) for the elements of the amplitude scattering matrix are valid provided that $k_1 r \gg 1$ and $k_1 r \gg n_{\rm max}^2$, where $n_{\rm max}$ is the maximal value of the summation index n in Eq. (5.3). Extensive practical T-matrix computations for single-body and aggregated scatterers suggest indeed that in order to achieve convergence for particles comparable to and greater than the wavelength, $n_{\rm max}$ must be equal to or slightly exceed x, which leads to $k_1 r \gg x^2$.

The above conclusion remains valid for the Lorenz–Mie theory since the latter is a particular case of the T-matrix method.

Acknowledgments

I thank Richard Chang, Bo Gustafson, Daniel Mackowski, and Gorden Videen for useful discussions and suggestions. This research was sponsored by the NASA Radiation Sciences Program managed by Hal Maring.

References

[1] Müller C. Foundations of the mathematical theory of electromagnetic waves. Berlin: Springer; 1969.
[2] Van de Hulst HC. Light scattering by small particles. New York: Dover; 1981.
[3] Mishchenko MI, Travis LD, Lacis AA. Scattering, absorption, and emission of light by small particles. Cambridge: Cambridge University Press; 2002 (available in the pdf format at http://www.giss.nasa.gov/~crmim/books.html).
[4] Hansen JE, Travis LD. Light scattering in planetary atmospheres. Space Sci Rev 1974;16:527–610.
[5] Ishimaru A. Wave propagation and scattering in random media. New York: Academic Press; 1978.
[6] Dolginov AZ, Gnedin YuN, Silant'ev NA. Propagation and polarization of radiation in cosmic media. Basel: Gordon and Breach; 1995.
[7] Mishchenko MI, Hovenier JW, Travis LD, editors. Light scattering by nonspherical particles: theory, measurements, and applications. San Diego: Academic Press; 2000.
[8] Liou KN. An introduction to atmospheric radiation. San Diego: Academic Press; 2002.
[9] Kahnert FM. Numerical methods in electromagnetic scattering theory. JQSRT 2003;79/80:775–824.

[10] Babenko VA, Astafyeva LG, Kuzmin VN. Electromagnetic scattering in disperse media: inhomogeneous and anisotropic particles. Chichester, UK: Praxis; 2003.
[11] Hovenier JW, Van der Mee C, Domke H. Transfer of polarized light in planetary atmospheres—basic concepts and practical methods. Dordrecht, The Netherlands: Kluwer; 2004.
[12] Mishchenko MI. Vector radiative transfer equation for arbitrarily shaped and arbitrarily oriented particles: a microphysical derivations from statistical electromagnetics. Appl Opt 2002;41:7114–34.
[13] Mishchenko MI. Microphysical approach to polarized radiative transfer: extension to the case of an external observation point. Appl Opt 2003;42:4963–7.
[14] Mishchenko MI, Hovenier JW, Mackowski DW. Singe scattering by a small volume element. J Opt Soc Am A 2004;21:71–87.